Horizontal Confinement of a Melamine Formaldehyde Dust Particle in an Argon Plasma

A Major Qualifying Project Report: Submitted to the Faculty of the
WORCESTER POLYTECHNIC INSTITUTE
in partial fulfillment of the requirements for the
Degree of Bachelor of Science
by
Autumn D. Paro
Advisors: Professor Germano Iannacchione and Professor Alex Zozulya

April 2012

ABSTRACT

This project focused on the how the horizontal confinement of a dust particle in a laboratory plasma changes based on pressure and cutout size. When a cutout is placed on the bottom electrode of a GEC reference cell, a potential well is created due to the change in the shape of the electric fields within the sheath. This provides the horizontal forces needed to restrict the particle from falling off the edge of the lower electrode.

Using different MATLAB programs, a single dust particles position was tracked though several frames, converted from pixels to meters, and used to determine the potential energy. A quadratic curve was then fitted to the potential versus time graph to determine the confinement coefficient κ on the x^2 term.

From the data analysis, it was determined that the potential energy assumes a parabolic form, which agrees with different proposed theories. It was also determined that κ increases proportionally as pressure increases for the $1/4$ inch cutout, which also agrees with theory.

CONTENTS

LIST OF FIGURES

1. PROBLEM STATEMENT

Complex (dusty) plasmas are partially ionized gases containing micrometer sized particles. Dusty plasmas account for the majority of plasmas within the universe and can be found in a variety of different places: interstellar clouds, planetary ring systems, and a variety of laboratory plasmas. Within laboratory plasmas such as the surface processing industry and high energy fusion reactors, the presence of dust is significant because it causes instabilities within the plasmas and damage to the equipment. In order to better understand the nature of the plasma-dust interactions, this project will study the horizontal confinement of dust particles within a low temperature argon plasma. A better understanding of the horizontal forces on a particle will provide a better understanding of how dust crystal lattices form and how it changes depending on the plasma parameters.

2. BACKGROUND

2.1 Plasmas

Throughout the universe there are four types of matter: solids, liquids, gases, and plasmas. According to Big Bang Theory, the universe began as a small hot dense ball that was unstable. When it exploded it began expanding, and some of the plasma cooled to gas, which then cooled to liquids, and eventually cooled to solids [5]. The fourth state of matter, plasma, is the least common on earth but the most common throughout the universe. It can be found in a variety of places such as the sun, stars, lightning, Aurora Borealis, Saturn's rings, solar wind, and other astrophysical bodies[5, 6, 7].

Plasma is an ionized gas that contains ions, electrons, and neutral atoms. Just like when a substance transitions from solid to liquid, or liquid to a gas, a phase transition occurs between the gas and plasma states. One of the differences between plasma and the other states of matter is that a plasma is comprised of charged particles as shown in figure 2.1. To transition from a gaseous state to a plasma state, energy is required to excite the particles. As the particles become more excited they move faster, colliding into one another. These collisions excite electrons to higher energy states, requiring little energy from the next collision to
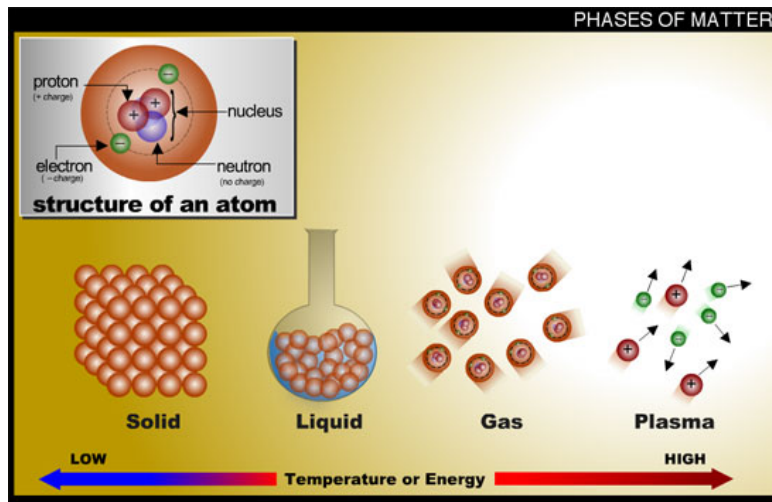
Fig. 2.1: Visual representation of the different states of matter and their transitions over temperature [1]. The plasma shown is fully ionized thus it only contains ions and electrons. Many plasmas are not fully ionized and contain neutral atoms as well.

release an electron, leaving a positive ion and a free electron. Two common ways of providing energy is to increase the temperature of the gas to between 3eV and 25eV or by sending an electric pulse through the gas. Unlike the other states of matter, plasma is able to interact internally with itself. Since each charged particle has its own electromagnetic field, the particle's fields and orbits affect each other concurrently [5, 7, 8, 9, 10].

When a gas is first ionized, the particles begin to move at a speed based on their mass and temperature. Since the ions are more massive than the electrons they move at a significantly slower speed. Because of this difference there are more collisions between electrons and the walls of the chamber, causing a net negative charge to build up. The positive ions are then attracted to the walls, thus a positive space charge forms around the edge of the walls. Once an equilibrium

state is reached, there are two distinct regions of the plasma.
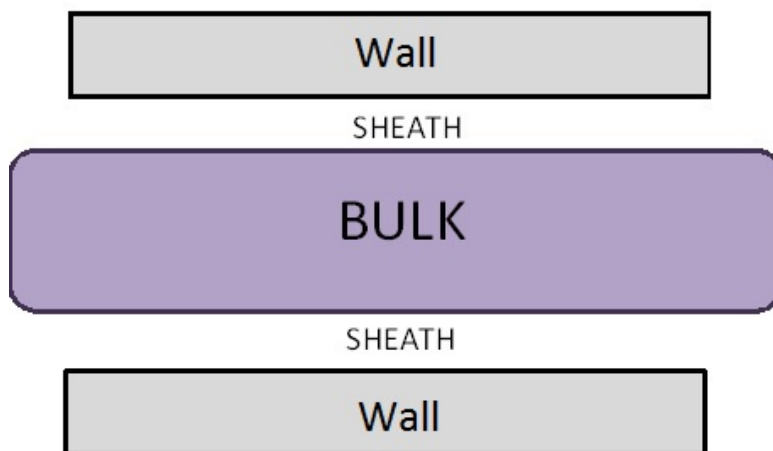
Fig. 2.2: Image of how the plasma interacts with its surrounding walls.

The two different regions of the plasma are called bulk and the sheath. The bulk is the main glowing area shown in figure 2.2. It has the highest density of ions and electrons and is where the majority of ionization occurs. The second area is called the sheath and consists of the dark region between the bulk and the containment walls. The sheath is created when the electrons move to prevent external electromagnetic forces from interacting with the bulk. Within the sheath, the number densities of the ions and electrons are not equal, causing the electric potential energy to increase monotonically from the negative value on the wall to a positive value within the bulk [9, 11].

2.2 Dusty Plasmas

Most plasmas found throughout the universe contain dust and are therefore classified as dusty (complex) plasmas. Dusty plasmas are partially ionized gases which contain micrometer sized particles. Occurring naturally in space, they had a large effect on the formation of the solar system [12, 13].

Scientists are fascinated by dusty plasmas because they occur naturally in extraterrestrial bodies and model other phenomena, such as crystals, found in nature. In a laboratory however, plasmas play a different role. The formation of dust within a plasma causes many issues because dust obtains a rather large negative charge. Since the electrons move much faster than the heaver ions, there are more collisions between electrons and the dust particles. This causes the dust to collect more free electrons than ions, altering the ion/electron ratio. If too much dust is present then the change in the ratio affects the ion/electron temperatures, plasma potential energy, and electromagnetic field within the chamber [13].

2.3 GEC Reference Cell

A Gaseous Electronics Conference (GEC) radio frequency (RF) reference cell is a common environment used to run low temperature plasma experiments. Since plasma characteristics are based on the geometry of their environment it was important that different labs had a similar geometry to allow for fair comparison of their data. At the 1988 Gaseous Electronics Conference it was agreed that a common geometry was required, and as a result the GEC RF reference cell was
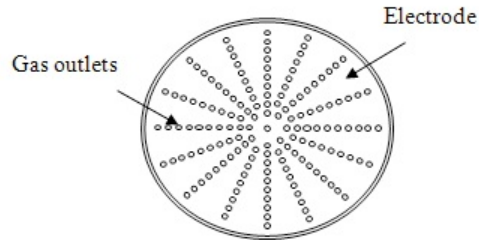
created in March 1989 [14, 4, 3].

Fig. 2.3: Top view of the upper electrode for the original GEC reference cell. This electrode contains little holes, mimicking a shower head, that act as gas outlets for the cell [2].

Figure 2.4 shows the basic design of the GEC reference cell decided on at the March 1989 meeting. The main part of the cell is the vacuum chamber, which contains two parallel plate electrodes. The lower electrode is connected to an RF amplifier and the upper electrode, called a shower electrode, is grounded. The upper electrode is called a shower head electrode, Figure 2.3, because it is mostly solid with small holes through it. There are four equally spaced viewing areas around the cell. The vacuum chamber is connected to two different types of pumps, a high vacuum pump and a mechanical pump. The high vacuum pump is turned on when the cell is not being used, which cleans the cell by preventing contaminants from sticking to the walls. During experiments the high vacuum pump is turned off, the gate valve is closed, and the mechanical pump is used. A throttling valve, connected to the mechanical pump and gas canister, is used to control the gas flow during the experiments.
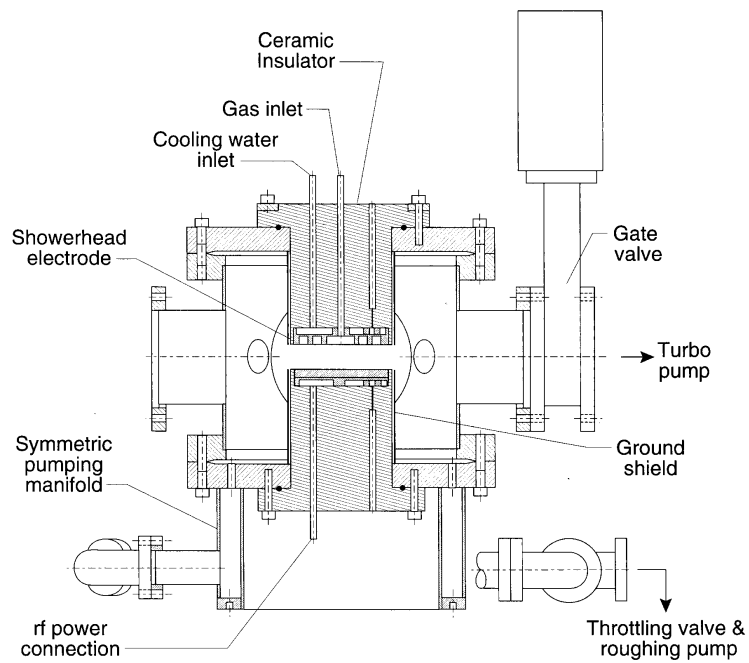
Fig. 2.4: Schematic of the GEC RF reference cell decided on in March 1989 [3].

3. THEORY

Dust particles within plasmas are exposed to a variety of forces in both the horizontal and vertical directions. While dust particles move through the plasma, they obtain a negative charge proportional to their size and location within the plasma. As they approach the lower sheath, the electrostatic force within the sheath cancels out the gravitational force, causing the dust to levitate in the sheath. Other forces that are present, but neglected for this experiment, are ion drag and thermophoretic forces.

If only one particle is present within the plasma, there are no forces in the horizontal direction, and the particle's random motion will eventually cause it to fall off the edge of the lower electrode. If several particles are present within the plasma they repel each other, and fall off the edge of the lower electrode at a faster rate. In order to contain the particles in this direction, a shallow circular well called a cutout is placed on top of the lower electrode. The presence of the cutout changes the shape of the sheath creating a weaker electric field in the horizontal direction which contains the particle. Since the sheath conforms to the shape of the lower electrode, it takes the form of a shallow bowl due to the cutout, which is why the potential is called a well [15]. It is assumed that this well takes on a

parabolic shape, though little has been found to prove or disprove this [16, 17]. In order to determine the shape of the potential energy we have to look at the particles equations of motion

$$m_d\ddot{x} + R\dot{x} - \frac{dU}{dx} = \begin{cases} 0 & \text{laser off} \\ \\ F_{laser} & \text{laser on} \end{cases} \qquad (3.1)$$

where m_d is the mass of the dust particle's mass, R is the drag coefficient, and U is the potential energy. Solving the potential energy for when the laser is off gives

$$U\left(x\left(t\right)\right) = U_0 - \frac{m_d\dot{x}^2}{2} - R\int_1^t \dot{x}^2(\tau)d\tau. \qquad (3.2)$$

which is the potential energy as a function of position. To simplify calculation the x-axis is aligned parallel to the path of the particle reducing the equation to one dimension the potential energy at $x = 0$, is set to $U_0 = 0$, leaving the drag coefficient R as the only unknown. The gas drag coefficient

$$R = m_d\beta \qquad (3.3)$$

is a constant that is dependent on the plasma parameters through the Epstein drag coefficient β. The Epstein drag coefficient

$$\beta = \frac{8}{\pi}\frac{P}{\rho a v_{th,n}} \qquad (3.4)$$

changes based on the plasma pressure P, the radius of the particle a, the density of the dust particle ρ, and the thermal velocity $v_{th,n}$ of the neutral gas[18]. The thermal velocity

$$v_{th,s} = \sqrt{\frac{k_B T_s}{m_s}} \qquad (3.5)$$

determines the speed at which ionized particles move when first ionized. Once the plasma is ionized the particles move based on their interactions with the surrounding particle. In this equation the subscript s stands for the possible particles, ions, electrons, and neutral particles, found in the plasma. If the ions and electrons had the same temperature, the ions will move at a much slower speed than the electrons since they are more massive which is shown in equation 3.5.

4. EXPERIMENTAL SETUP

The experiment for determining the shape of the potential well was run using a modified GEC RF reference cell located in the Baylor University Center for Astrophysics, Space Physics, and Engineering Research lab. The cell used, shown in figure 4.1, is very similar to the one decided on at the 1989 meeting, with slight variations. Instead of using a showerhead electrode, figure 2.3, this cell uses a hollowed upper electrode, figure 4.2. Four 6-inch diameter viewing ports are placed around the cell, with a fifth placed above the upper electrode. Two CCD cameras, one located above the upper electrode and one at one of the side ports, are used to obtain top and side views of the plasma simultaneously. Each camera is paired with a low-powered diode laser used to illuminate the dust as shown in figure 4.3 [2]. The horizontal diode laser is focused into a horizontal sheet while the vertical laser has is focused into a vertical sheet.

Before running this experiment, the electrode spacing was set to 1 inch and using an rf amplifier, argon plasma was ignited. After the plasma was ignited, a single $8.8 \mu m$ melamine formaldehyde dust particle was dropped into the plasma using the dust shaker positioned above the upper electrode. Once the particle settled in its equilibrium position, it was pushed away from the center using radiation
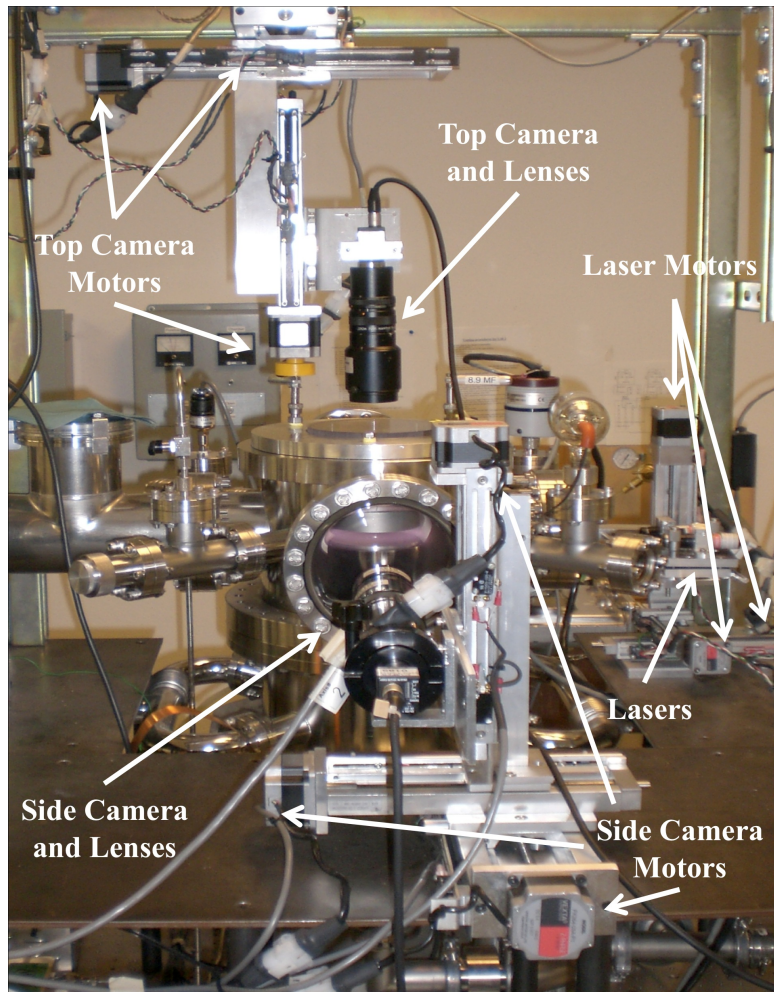
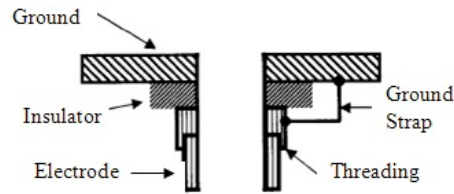*Fig. 4.1:* Image of the GEC reference cell used at in the CASPER lab [2].

Fig. 4.2: Schematic of the upper electrode used in the CASPER cell. The hollowed nature allows for optical measurements to be taken from above [2].

pressure from a variable power Verdi laser $(0-5W)$, not shown in figure 4.3. This laser was focused down to a small spot in order to push the particle away from its equilibrium position. When the laser was turned off the particle returned to the equilibrium position. Using a 60 FPS camera, the particle's trajectory was tracked while the laser was pushing it and on its return trip to equilibrium. The experiment was repeated for two different cutout sizes, seven different pressures, and two different voltage DC (VDC) values. The VDC is the voltage applied to the lower electrode to keep the voltage fixed.
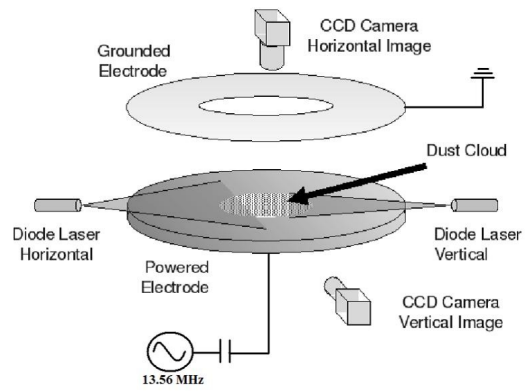
Fig. 4.3: Schematic of how the cameras and lasers pair up to illuminate the dust [4].

5. METHODS

Using a computer program I tracked the particle's position through each of the frames for each run. The code cropped the image to a specified area and a minimum brightness threshold was set. Once this was done the center of the particle was determined and the pixel location of the center was recorded for each frame. Once the particles position was determined in pixels, it was converted to meters. Both data sets had a frame rate of $60\,frames/s$, however they had different pixel sizes. The first data set had a pixel size of$15.95\mu m$, while the second had a pixel size of $30\mu m$. After the position was determined in meters, the position versus time was plotted, the areas of interest shown in figure 5.1 were isolated. At this point the position was differentiated to determine the particles position which was then used to find $\int_{0}^{t} v^2(\tau)d\tau$. Using $75, 100, 125, 150, 200, 250,$ and $300mTorr$ for the pressure values, equations 3.3, 3.4, 3.5 were used to determine the drag coefficient R. Putting this data back into equation 3.2 the potential as a function of position was found. Using a curve fitting tool a quadratic curve was fitted to the data and the confinement coefficient κ was obtained from the coefficient on the x^2 term. This was done for about ten runs at each setting and the values obtained for κ at each setting were averaged.
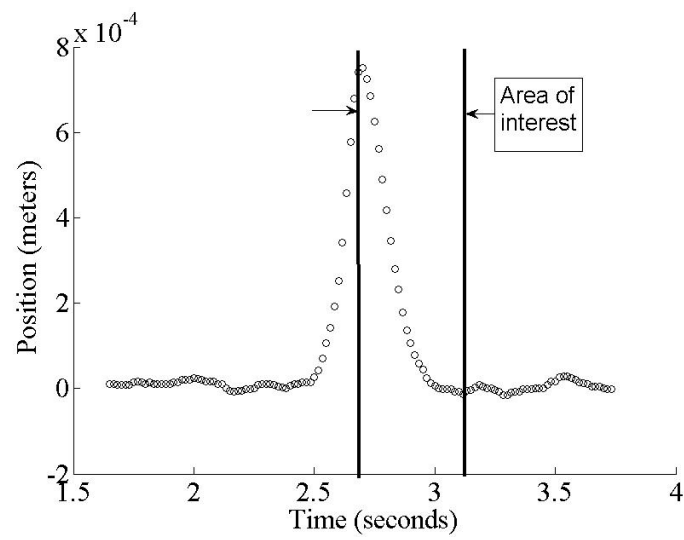
Fig. 5.1: Particle trajectory while under the influence of the laser and on its return trip with the area of interest highlighted.
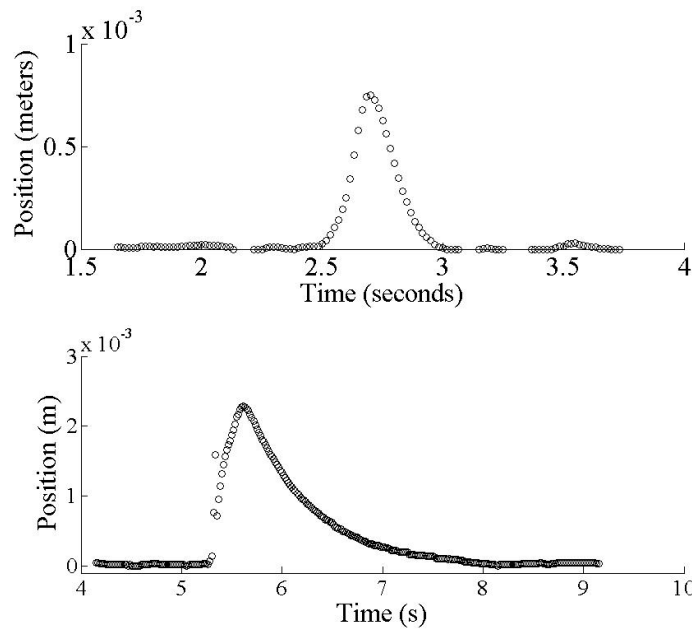
6. RESULTS AND DISCUSSION

Fig. 6.1: Positions as a function of time for the two different cutout sizes, a) $1/4$inch b) 1inch, at 100mTorr Pressure and -7 VDC. The solid line is the fitted quadratic equation describing the shape of the data.

Figure 6.1 shows the positions versus time for a single particle at 100mTorr, -7 VDC, and both the $1/4$ inch and 1 inch cutouts. In Figure 6.1(a) the 30mW Verdi laser was turned on at 2.5 seconds and was switched off at about 2.75 seconds. The return trajectory takes the shape of an exponential decay until the particle reaches

its equilibrium position at about 3 seconds when it becomes constant. For figure 6.1(b) the laser was turned on just after the 5 seconds mark and switched off just before the 6 seconds mark. Again, the trajectory takes the form of an exponential decay, though it takes longer to reach its equilibrium position at approximately 8 seconds. The exponential decay comes from the equations of motion which are damped due to the drag forces proportional to the thermal velocity of the particles. For each of the different settings the return has the form of an exponential decay, though it takes longer for particles in the 1 inch cutout to return to equilibrium, as shown in Figure 6.1.

As the distance between the particle and the edge of the cutout increases, the force on the particle will decrease, causing the acceleration to decrease. Since the 1 inch cutout has a larger radius, there is more distance for the particle to travel from the equilibrium point to the edge of the cutout. This gives a larger distance between the particle and the edge, decreasing the force acting on the particle. The smaller force contributes to a slower acceleration and thus the smaller slope found in 6.1(b) compared to the slope in 6.1(a).

The potential energy versus position graphs shown in Figure 6.2 shows how the potential energy changes based on the particles position for a sample of the 1 and $1/4$ inch cutouts. As the two graphs show, the potential energy has a parabolic shape which agrees with literature [16, 17]. The potential energy was found to be parabolic for each setting used, but the confining coefficient, κ, which determines the steepness of the parabola, varied between settings. Figure 6.4 shows how the confining coefficient, κ, changes based on pressure for the two different cutout
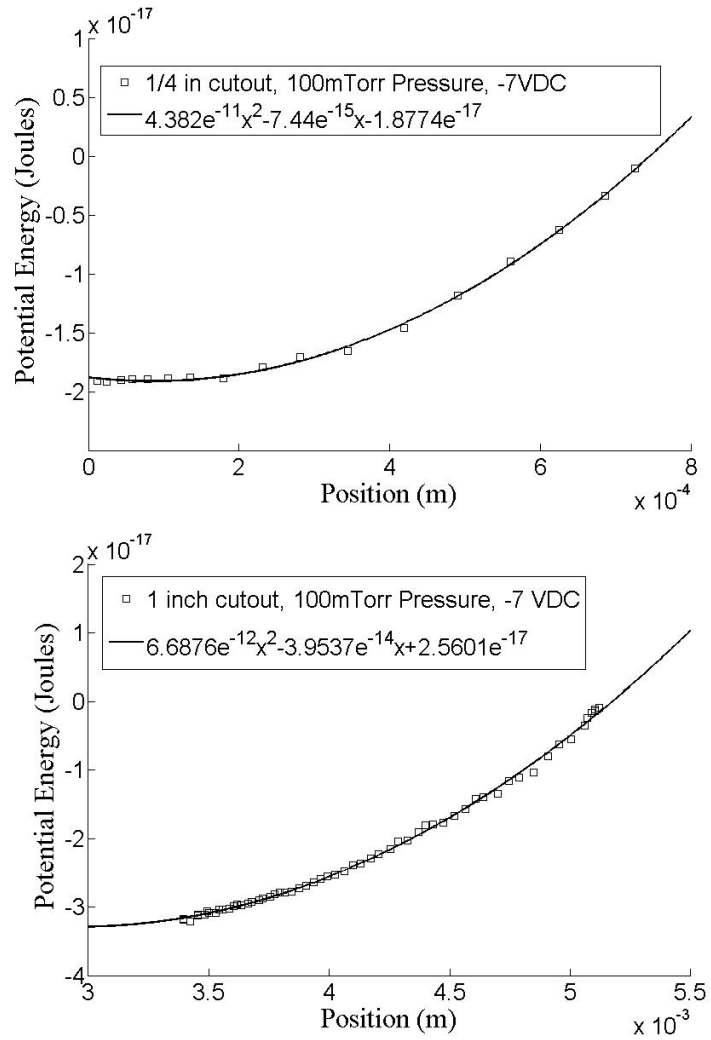
Fig. 6.2: Potential Energy as a function of position for the two different cutout sizes, a) 1/4inch b) 1inch, at 100mTorr Pressure and -7 VDC
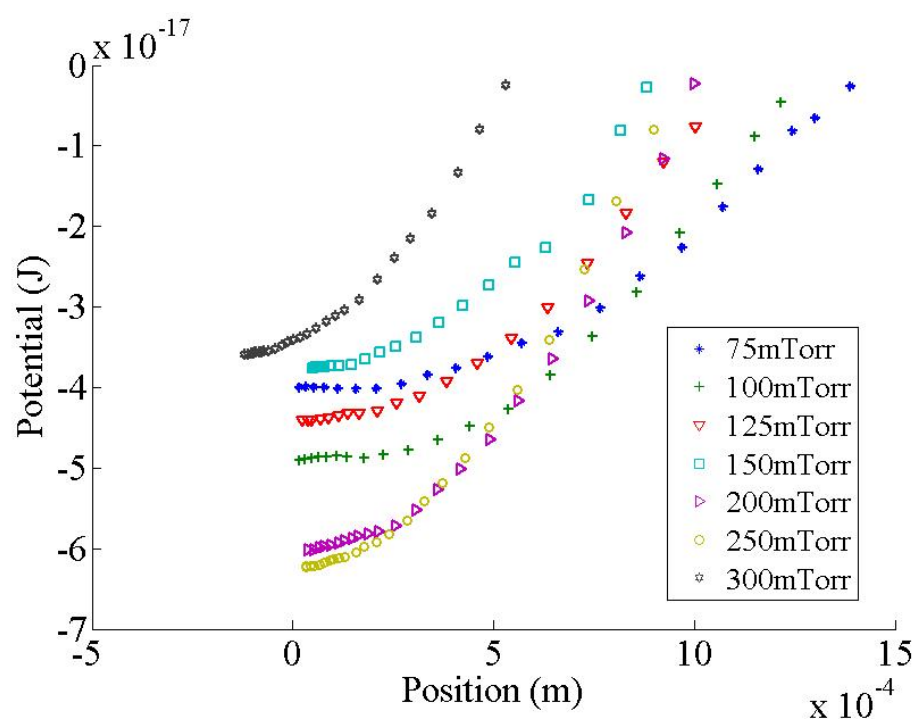
Fig. 6.3: Potential Energy as a function of positions for the six different pressures and the 1/4 inch cutout at -7 VDC.
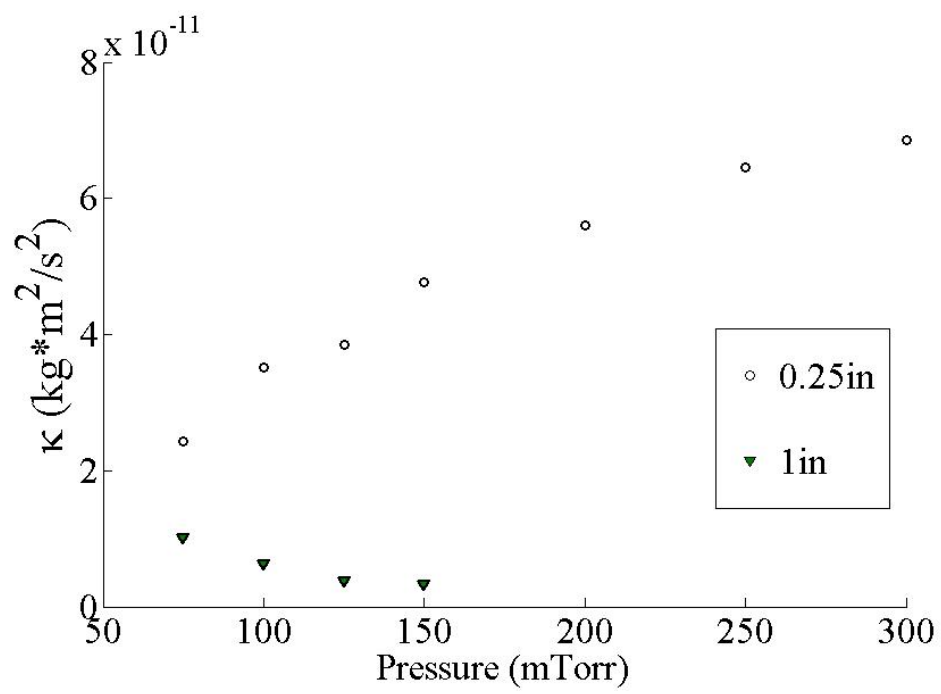
Fig. 6.4: Confining coefficient as a function of pressure for the 1/4 and 1 inch cutouts at -7 VDC.

sizes. For the small cutout κ increases as pressure increases. As seen in Figure 6.3, the absolute value of the potential energy typically increases as pressure increases with a few outliers such as the 300mTorr and the 150mTorr. For the 1 inch cutout, the confining coefficient decreases as the pressure increases. This does not agree with the other papers or the theory. The discrepancy in this data could be due to the small data set that was used.

6.1 Future Work

For future work on this project, additional settings as well as a larger variation on the setting currently being used. Possible settings to look into are cutout size, the glass box, pressure, and VDC.

BIBLIOGRAPHY

[1] URL. Sun-earth connection. April 2006. *http//www.nasa.gov/mission_pages/themis/auroras/sun_earth_connect.html*.

[2] James Ruell Creel. Characteristic measurements within a gec rf reference cell, 2010.

[3] J. K. Olthoff and K. E. Greenberg. The gaseous electronics conference rf reference cell-an introduction. *J. REs. Natl. Inst. Stand. Technol.*, 100:327–339, 1995.

[4] Victor Land, Erica Shen, Bernard Smith, Lorin Matthews, and Truell Hyde. Experimental and computational characterizatoin of a modified gec cell for dusty plasma experiments.

[5] Yaffa Eliezer and Shalom Eliezer. *The Fourth State of Matter: An Introduction to the Physics of Plasma*. 1 edition, 1989.

[6] M. Horanyi, T. W. Hartquist, O. Havnes, D. A. Mendis, and G. E. Morfill. Dusty plasma effects in saturn's magnetosphere. *Reviews of Geophysics*, 42:RG4002, 2004.

[7] Martin A. Uman. *Introduction to Plasma Physics*. 1 edition, 1964.

[8] Dwight R. Nicholson. *Introduction to Plasma Theory*. John Wiley & Sons, Inc., 1 edition, 1983.

[9] Umran Inan and Marek Golkowski. *Principles of Plasma Physics for Engineers and Scientists*. 1 edition, 2011.

[10] Alexander Piel. *Plasma Physics: An Introduction to Laboratory, Space, and Fusion Plasmas*. Springer, 1 edition, 2010.

[11] S. R. Seshadri. *Fundamentals of Plasma Physics*. American Elsevier Publishing Company Inc., 1 edition, 1973.

[12] Patrick Ludwig, Michael Bonitz, and Jurgen Meichsner. *Introduction to Complex Plasmas*. Springer-Verlag Berlin Heidelberg, 1 edition, 2010.

[13] S.V. Vladimirov, K. Ostrikov, and A. A. Samarian. *Physics and Applications of Complex Plasmas*. Imperial College Press.

[14] M. L. Brake, J. Pender, and J. Fournier. The gaseous electronics conference (gec) reference cell as a benchmark for understanding micrelectronics processing plasmas. *Physics of Plasmas*, 6:2307–2313, 1999.

[15] Bin Liu, J. Goree, V. Nosenko, and L. Boufendi. Radiation pressure and gas drag forces on a melmine-formaldehyde microsphere in a dusty plasma. *Physics of Plasmas*, 10:9–20, 2003.

[16] G.A. Hebner, M. E. Riley, D. S. Johnson, Pauline Ho, and R. J. Buss. Direct determination of particle-particle interactions in a 2d plasma dust crystal. *Physical Review Letters*, 87:235001–1–235001–4, 2001.

[17] U. Konopka, G.E. Morfill, and L. Ratke. Measurement of the interaction potential of microspheres in the sheath of a rf discharge. *Physical Review Letters*, 84:891–894, 2000.

[18] Zhuanhao Zhang, Ke Qiao, Jie Kong, Lorin Matthews, and Truell Hyde. Simple method to measure an interaction potential of dielectric grains in a dusty plasma. *Physical Review E*, 82:036401–1–036401–7, 2010.